

See discussions, stats, and author profiles for this publication at: <https://www.researchgate.net/publication/227656011>

Mapping abandoned agriculture with multi-temporal MODIS satellite data

Article in Remote Sensing of Environment · September 2012

DOI: 10.1016/j.rse.2012.05.019

CITATIONS

126

READS

277

4 authors, including:



Pedro Camilo Alcantara Concepcion

Universidad de Guanajuato

28 PUBLICATIONS 835 CITATIONS

[SEE PROFILE](#)



Tobias Kuemmerle

Humboldt-Universität zu Berlin

250 PUBLICATIONS 7,057 CITATIONS

[SEE PROFILE](#)



Volker Radeloff

University of Wisconsin-Madison

328 PUBLICATIONS 11,121 CITATIONS

[SEE PROFILE](#)

Some of the authors of this publication are also working on these related projects:



PASANO- Pathways to sustainable land management in Northern Argentina [View project](#)



Protected area effectiveness in the Caucasus during socioeconomic and political shocks [View project](#)



(This is a sample cover image for this issue. The actual cover is not yet available at this time.)

This article appeared in a journal published by Elsevier. The attached copy is furnished to the author for internal non-commercial research and education use, including for instruction at the authors institution and sharing with colleagues.

Other uses, including reproduction and distribution, or selling or licensing copies, or posting to personal, institutional or third party websites are prohibited.

In most cases authors are permitted to post their version of the article (e.g. in Word or Tex form) to their personal website or institutional repository. Authors requiring further information regarding Elsevier's archiving and manuscript policies are encouraged to visit:

<http://www.elsevier.com/copyright>

Contents lists available at [SciVerse ScienceDirect](http://www.sciencedirect.com)

Remote Sensing of Environment

journal homepage: www.elsevier.com/locate/rse

Mapping abandoned agriculture with multi-temporal MODIS satellite data

Camilo Alcantara^{a,*}, Tobias Kuemmerle^{b,c}, Alexander V. Prishchepov^d, Volker C. Radeloff^d^a Facultad de Ciencias Naturales, Universidad Autónoma de Querétaro, Antiguo Aeropuerto, Carr. Chichimequillas s/n. Terreno Ejidal Bolaños, C.P. 76140, Querétaro, Mexico^b Geography Department, Humboldt-University Berlin, Unter den Linden 6, 10099 Berlin, Germany^c Earth System Analysis, Potsdam Institute for Climate Impact Research (PIK), P.O. Box 60 12 03, Telegraphenberg A62, D-14412 Potsdam, Germany^d Department of Forest and Wildlife Ecology, University of Wisconsin-Madison, 1630 Linden Drive, Madison, WI, 53706-1598, USA

ARTICLE INFO

Article history:

Received 17 May 2011

Received in revised form 17 May 2012

Accepted 19 May 2012

Available online xxxx

Keywords:

Agricultural abandonment

Change detection

Eastern Europe and the former Soviet Union

Fallow land

Farmland

Landsat

Land use and land cover change

MODIS

Phenology

Support vector machines

SVM

Time series

ABSTRACT

Agriculture is expanding and intensifying in many areas of the world, but abandoned agriculture is also becoming more widespread. Unfortunately, data and methods to monitor abandoned agriculture accurately over large areas are lacking. Remote sensing methods may be able to fill this gap though, especially with the frequent observations provided by coarser-resolution sensors and new classification techniques. Past efforts to map abandoned agriculture relied mainly on Landsat data, making it hard to map large regions, and precluding the use of phenology information to identify abandoned agriculture. Our objective here was to test methods to map abandoned agriculture at broad scales with coarse-resolution satellite imagery and phenology data. We classified abandoned agriculture for one Moderate Resolution Imaging Spectroradiometer (MODIS) tile in Eastern Europe (~1,236,000 km²) where abandoned agriculture was widespread. Input data included Normalized Difference Vegetation Index (NDVI) and reflectance bands (NASA Global MODIS Terra and Aqua 16-Day Vegetation Indices for the years 2003 through 2008, ~250-m resolution), as well as phenology metrics calculated with TIMESAT. The data were classified with Support Vector Machines (SVM). Training data were derived from several Landsat classifications of agricultural abandonment in the study area. A validation was conducted based on independently collected data. Our results showed that it is possible to map abandoned agriculture for large areas from MODIS data with an overall classification accuracy of 65%. Abandoned agriculture was widespread in our study area (15.1% of the total area, compared to 29.6% agriculture). We found strong differences in the MODIS data quality for different years, with data from 2005 resulting in the highest classification accuracy for the abandoned agriculture class (42.8% producer's accuracy). Classifications of MODIS NDVI data were almost as accurate as classifications based on a combination of both red and near-infrared reflectance data. MODIS NDVI data only from the growing-season resulted in similar classification accuracy as data for the full year. Using multiple years of MODIS data did not increase classification accuracy. Six phenology metrics derived with TIMESAT from the NDVI time series (2003–2008) alone were insufficient to detect abandoned agriculture, but phenology metrics improved classification accuracies when used in conjunction with NDVI time series by more than 8% over the use of NDVI data alone. The approach that we identified here is promising and suggests that it is possible to map abandoned agriculture at broad scales, which is relevant to gain a better understanding of this important land use change process.

© 2012 Elsevier Inc. All rights reserved.

1. Introduction

Agricultural change is a key component of Land Use and Land Cover Change (LULCC; Foley et al., 2005; Goldewijk & Ramankutty, 2004; Haberl et al., 2007; Leff, Ramankutty, & Foley, 2004; Tilman et al., 2001; Tilman, 1999). As of 2005, more than 38% of the Earth's land surface was either in row crops or grazed (Food and Agriculture Organization of the United Nations, 2010). Cropland alone has increased rapidly during the last centuries, occupying 3–4 million km² in 1700 and 15–

18 million km² in 1990 (about 12% of the global land surface) (Lambin & Geist, 2006; Leff et al., 2004). However, in recent decades, total area of agriculture stabilized or even decreased in several parts of the world; especially in the temperate zone (Lambin & Geist, 2006). Such reduction of total area of agriculture resulted mainly in abandoned agriculture, and sometimes concomitant increase in forest area (Kauppi et al., 2006; Millennium Ecosystem Assessment, 2005; Rudel et al., 2005). While agricultural expansion and associated deforestation are relatively well-documented though (Lambin & Geist, 2006), much less is known about the patterns, causes and the environmental consequences of abandoned agriculture (Aide & Grau 2004; Cramer, Hobbs, & Standish, 2008; Rey Benayas, Martins, Nicolau, & Schulz, 2007; Vandermeer & Perfecto, 2007).

* Corresponding author. Tel.: +52 442 286 3874; fax: +1 608 262 9922.
E-mail address: alcantara@wisc.edu (C. Alcantara).

Properly defining *abandoned agriculture* is not easy. Because abandoned agricultural areas are in transition, the land use change is without fixed patterns, and often non-linear (Lambin & Meyfroidt, 2011a, b). *Abandoned agriculture* is the result of a land owner's decision to reduce the intensity of use of land for agriculture (including grazing) for an undetermined period of time; based on either natural, socio-economic, or personal constraints. The decision to abandon an agricultural area can precede the actual abandonment by months or even years, depending on the type of agricultural use, and even more time can expire before abandoned agriculture can be detected via remote sensing. Vice versa, fallow periods are part of the typical crop rotation cycle, making it difficult to ascertain if a field has been truly abandoned or is just awaiting future use. However, as more time expires, it becomes more obvious that a field is abandoned, especially if shrubs and trees start to grow on former fields, since woody plants make it increasingly costly to start agricultural use again, and farmers will typically avoid woody growth on their fields.

Satellite imagery can provide independent and consistent data to map LULCC such as agricultural abandonment, if abandonment results in a unique land cover type or a unique land cover change trajectory (Fassnacht, Cohen, & Spies, 2006; Lu, Mausel, Brondizios, & Moran, 2004). In terms of its vegetation cover, abandoned agriculture follows a broadly repeatable progression of recovery from short-lived herbaceous species to longer-lived woody species such as shrubs and trees in areas where forests can grow. Ecologists call this trajectory, i.e., the recovery of forest growth after disturbance, succession. Succession occurs after any type of disturbance, and agricultural land use is simply a particularly severe form of disturbance in this context. However, while the general trajectory of succession is fairly predictable, the rate of succession, and the species composition at each stage of succession are highly dependent on prior land use and the colonization dynamics of both native and exotic species, which in turn, are strongly affected by the land use patterns in the surrounding of the abandoned agricultural field. Pre-disturbance plant communities are unlikely to recover if the legacy of cultivation is such that nutrient and water cycles are permanently altered, and the vegetation is highly fragmented (Cramer et al., 2008).

From a remote sensing perspective, the land use process of agricultural abandonment can be mapped in two ways. The first is change detection, in which case abandoned agriculture represents areas that are initially agriculture and successional grassland, scrubland or forest at a later point (Baumann et al., 2011; Kuemmerle et al., 2008; Prishchepov et al. in review), but this requires imagery dating back to the time before abandonment. The second approach is to map areas with fallow grasslands that have woody growth, since such areas are transitional in zones where forests represent the potential natural vegetation. In other words, agricultural land abandonment is a land use process, and abandoned agriculture is a unique land cover type that results from abandonment. Our research here was focused to address the question: What kind of data, and from how many years and image dates, are needed to correctly map abandoned agriculture as a unique land cover type?

For the purpose of our study, we thus defined abandoned agriculture as areas that (1) had been previously used either for row crops, hay cutting, or as grazing lands, (2) are no longer in use, (3) have not been used for a time period longer than fallow periods under typical crop rotations, and (4) are characterized by woody growth that has started to appear as a result of natural succession. Other land use change processes that lead to the loss of agricultural land, such as urban development, were not considered abandoned agriculture under this definition. Based on this definition, we mapped those areas that showed a specific spectral and phenological signature that corresponds to regrowth of woody vegetation on fields that had been previously used for agriculture including grazing.

Agricultural abandonment is not a new phenomenon. Expansion and contraction of the agricultural land area has been common

since the origins of agriculture (Ellis, Goldewijk, Siebert, Lightman, & Ramankutty, 2010; Ramankutty & Foley, 1999). However, recently, agriculture abandonment rates have risen globally (Kauppi et al., 2006), especially in parts of North America (Klooster, 2003; Ramankutty, Heller, & Rhemtulla, 2010), Europe (Baumann et al., 2011; Kuemmerle et al., 2008; Müller et al., 2009) and South America (Aide, Zimmerman, Herrera, Rosari, & Serrano, 1995; Farley, 2007). Most recently agricultural abandonment has occurred in temperate regions, but also in tropical countries such as Puerto Rico (Grau et al., 2003), Mexico (Klooster, 2003), Ecuador (Farley, 2007), Honduras (Redo, Joby Bass, & Millington, 2009), Panama (Sloan, 2008), and Vietnam (Meyfroidt & Lambin, 2008). However, reliable data on abandonment are missing for most countries (Herold, Mayaux, Woodcock, Baccini, & Schmullius, 2008; Lepers et al., 2005; Ramankutty et al., 2007).

Robust data on agricultural abandonment is important to obtain though, because abandonment has strong environmental implications, affecting, for example, soil stability, carbon sequestration, water quality and nutrient cycling (MacDonald et al., 2000; Moreira & Russo, 2007; Ramankutty et al., 2007; Stoate et al., 2001). Environmental benefits of agricultural abandonment can include less pollution by agricultural chemicals (Lesschen, Cammeraat, Kooijman, & Van Wesemael, 2008), and the creation of new wildlife habitat (Chauchard, Carcaillet, & Guibal, 2007; Russo, 2007). However, agricultural abandonment can also increase the risk of natural hazards (Romero-Calcerrada & Perry, 2004) and alter water resources (Poyatos, Latron, & Llorens, 2003). In economic and social terms, agricultural abandonment decreases food production, and threatens traditional landscapes, their cultures and the biodiversity connected to these landscapes (Dutch National Reference Center for Agriculture, Nature and Food Quality, Latvian Ministry of Agriculture, & Latvian State, 2005). Furthermore, interest in abandoned agricultural land is rapidly growing in light of a looming land scarcity due to the rapidly increasing demand for food, fiber and biofuel (Foley et al., 2011; Lambin & Meyfroidt, 2011a,b).

Because of the importance of abandonment as a land use change process, remote sensing has been widely used to map it. In the United States of America, remote sensing has focussed on mapping the abandoned agriculture from the Conservation Reserve Program (Egbert, Lee, Price, & Boyce, 1998; Egbert et al., 2002; Park & Egbert, 2008). In Europe, studies that mapped abandoned agriculture from satellite imagery were conducted in Italy (Falcucci, Maiorano, & Boitani, 2007), Denmark (Kristensen, Thenail, & Kristensen, 2004), Estonia (Peterson & Aunap, 1998), Belarus and Lithuania (Prishchepov et al., in review), and the Carpathians (Kuemmerle et al., 2008; Kuemmerle, Kozak, Radeloff, & Hostert, 2009; Baumann et al., 2011). In Asia, a study mapped abandoned agriculture in the Siberian part of Russia (Bergen et al., 2008). All of these investigations used Landsat images from multiple dates, separated at least by three years, and employed change detection algorithms to identify areas that were initially in agricultural use, and no longer used at a later point in time.

While these Landsat-based studies highlight that abandoned agriculture can be accurately mapped with satellite imagery, they also point to some shortcomings of current approaches. First, past efforts to map abandoned agriculture were spatially limited to relatively small case studies that cannot be easily compared because of different change detection algorithms, classification schemes, abandonment definitions, and images dates (Prishchepov et al., in review). Second, past efforts used typically one or two Landsat images for a given year. This is potentially limiting, because mapping abandoned agriculture is inherently complex. Even at fine resolution it is not easy to discriminate whether or not an area was actively farmed in a given year when looking only at one or two points in time during one growing period. However, it is possible to improve the classification accuracy by analyzing multitemporal data, especially data captured early and late during the growing period (Baumann et al.,

2011; Prishchepov et al., in review). The Landsat archive is now freely available, and that opens new opportunity to analyze Landsat time-series. However, the availability of cloud-free images is often limited and that makes it difficult to compile large image composites for multiple dates during the growing period.

Differences in phenology are key to separate abandoned agriculture from agricultural areas that remain in use. A recent study suggests that three Landsat images per year, both pre- and post-abandonment, are necessary to achieve classification accuracies up to 80%, but sufficient cloud free images are often not available (Prishchepov et al., in review). Landsat imagery may thus not be the best data source to map abandoned agriculture for large areas. In contrast, coarse-resolution satellite imagery may offer advantages in terms of both spatial and temporal coverage with their ability to capture phenology (White et al., 2008; Xiao, Hagen, Zhang, Keller, & Moore, 2006; Zhang, Friedl, Schaaf, & Strahler, 2005), but their ability to map abandoned agriculture has not been tested.

The most common satellite sensors used to map LULCC at broad scale have been the Advanced Very High Resolution Radiometer (AVHRR), the VEGETATION sensor aboard Satellite Pour l'observation de la Terre (SPOT), and the Moderate Resolution Imaging Spectroradiometer (MODIS, Friedl et al., 2002, Fensholt & Sandholt, 2005). MODIS has two bands that can be used to map abandoned agriculture and are spectrally equivalent to the Landsat bands for red and near infra-red, but at 250-m resolution. Additionally, phenology metrics, such as start, end, middle and length of the growing period over broad scale images have been used to map land cover with good results (Jacquin, Sheeren, & Lacombe, 2010). Abandoned agriculture has a distinct phenological profile

compared to other land-cover types. Abandoned agriculture maintains a high NDVI value longer during the growing period than active agricultural lands and grasslands, but not as long as young and mature forests (Fig. 1). However, it is not clear how temporally high- but spatially coarse-resolution satellite imagery can be best analyzed to map abandoned agriculture.

Land-cover classifications from MODIS-type imagery are typically most accurate when using non-parametric, machine-learning algorithms, such as neural networks (Justice et al., 2002), or decision trees (Friedl & Brodley, 1997). Among the machine learning algorithms, support vector machines (SVMs) have shown particular promise when applied to Landsat data (Hermes, Friauff, Puzicha, & Buhmann, 1999, Kuemmerle et al., 2009), including agricultural abandonment classifications (Kuemmerle et al., 2008, Prishchepov et al., in review). For broad-scale mapping SVMs have been used successfully to predict Gross Primary Productivity (GPP) for the conterminous U.S. (Yang et al., 2007). However, coarse-resolution land-cover classification with SVMs are rare, although a case study classifying land cover from MODIS in Portugal shows promises (Goncalves, Carrão, Pinheiro, & Caetano, 2005).

Our goal here was to evaluate which combination of satellite and phenological data results in the best classification of abandoned agriculture at broad scales with coarse-resolution MODIS vegetation index (VI, 250 m) satellite imagery using SVMs as a classification method. Specifically, we tested different combinations of near-infrared (NIR) and red reflectance data, normalized difference vegetation indices (NDVI) data, and phenology metrics in order to map abandoned agriculture.

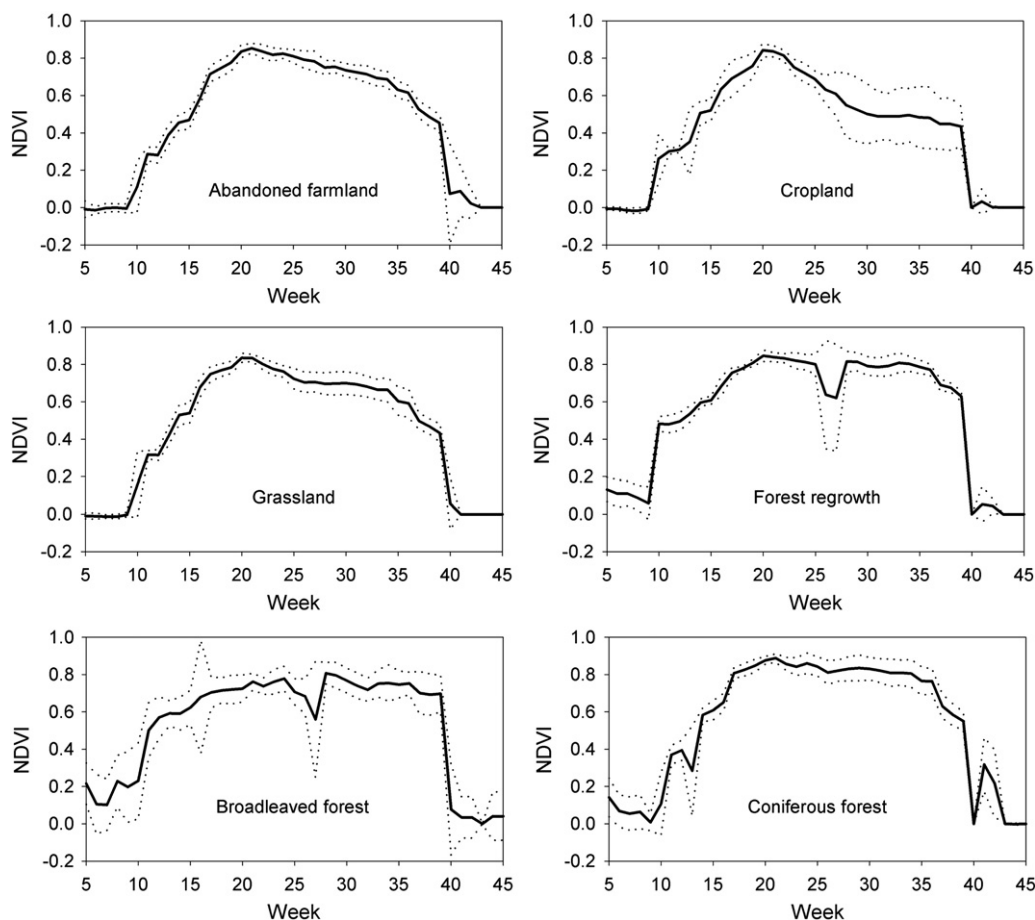


Fig. 1. Examples of MODIS NDVI time-series for the main land cover types that we classified for study area. We selected 10 pure pixels for each land cover type, according to our Landsat classifications, and verified the land cover type based on Google Earth imagery. The dotted envelopes represent the maximum and minimum NDVI values at each point in the time-series.

2. Methods

2.1. Eastern Europe study area

We classified MODIS VI 250-m resolution data from 2003 to 2008 to detect abandoned agriculture in the Baltic countries, Belarus and Poland (Fig. 2a and b). The study area encompassed 12,364,340 km², the extent of one MODIS tile (h19-v03) covering the entire area of Lithuania, Latvia, Estonia and Belarus, 77.4% of Poland, 18.4% of Ukraine, 8.4% of Czech Republic, and 2.1% of Russia (however, the Russian portion of the study area, including Kaliningrad, was larger than Poland) (Fig. 2b). This part of Eastern Europe was ideal for our study questions, because abandoned agriculture became widespread after the collapse of the USSR (Kuemmerle et al., 2008; Prishchepov et al., in review; Charles, 2010; Nikodemus, Bell, Grine, & Liepins, 2005; Peterson & Aunap, 1998).

The entire study area was glaciated several times and the Last Glacial Maximum was approximately 20,000 years ago. As a result, topographic variation is low (0–290 m) (Zeeberg, 1998). The dominant soils in the study area are arenosols, phaeozems, fluvisols, cambisols and luvisols. Podzols, which are poorly suited for agriculture, are widespread in the region as well, especially in the north. The climate is characterized by moist, cloudy, and cool summers and relatively mild winters. Frost free periods range from 150 to 179 days in the northeast to 210 to 240 days in the south. Average temperatures in July are 20 to 25 °C and average temperature in January is –3 to –5 °C. Annual precipitation ranges from 500 mm in central Poland to 900 mm in the mountains between Poland and the Czech Republic. Forests are boreal in the north (dominant tree species include *Pinus sylvestris*, *Picea abies*, and *Betula* spp.) and temperate in the south (dominant tree species include *Quercus* spp., *P. sylvestris*, and *P. abies*).

The majority of the agricultural abandonment in the study area occurred during the 1990s, right after the collapse of the USSR (Prishchepov et al., in review). MODIS data are only available after 2001 though, and can thus not be used for actual change detection

(i.e., the mapping of areas that were farmed during USSR times and covered by secondary succession later). Instead, we used the MODIS data to map abandoned agriculture, i.e., areas covered by secondary succession such as grasses that were neither mowed nor grazed, shrubs, and in some cases young trees. Whether or not these areas were indeed farmed during the USSR regime (pre-1991) was verified with 1980s Landsat imagery for a sample of sites (see below).

2.2. Input data for the classifications

We based all of our classifications on the two MODIS Vegetation Indices datasets (MODIS Terra and Aqua VI) 16-Day L3 Global Collection 5.0 (MOD13Q1 and MYD13Q1) from January 1, 2003 to December 31, 2008 (231.65 m resolution, or 5.36 ha). Data was retrieved from the Land Processes Distributed Active Archive Center (LP DAAC, <http://lpdaac.usgs.gov>) on August 31, 2009. The combined MODIS VI dataset includes weekly reflectance, NDVI, and quality data. We analyzed 250-m 16-day red reflectance data, 250-m 16-day near-infrared reflectance data, and 250-m 16-day normalized difference vegetation index (NDVI) data, each of which is available for 46 dates per year, from both Terra and Aqua datasets.

To identify the best year or years for our analysis, we examined the amount of MODIS Nadir BRDF (bidirectional reflectance distribution function) adjusted reflectance data available in different quality classes in each year for the red and infrared bands (Science Data Sets for MODIS Terra + Aqua BRDF/Albedo Quality 16-Day L3 Global 500-m SIN Grid V005, MCD43A2). Because of limited availability of usable data (categories 1–3) for the early years of the MODIS data record, we restricted our analysis to 2003–2008. Furthermore, 2005 and 2006 were the years with the most reflectance data in the ‘best’ quality category, and this is why we focused in some of our tests on these two years.

Phenology metrics can improve land-cover classifications from coarse-resolution satellite imagery (Jacquin et al., 2010). To identify whether or not phenology metrics can be used to map abandoned

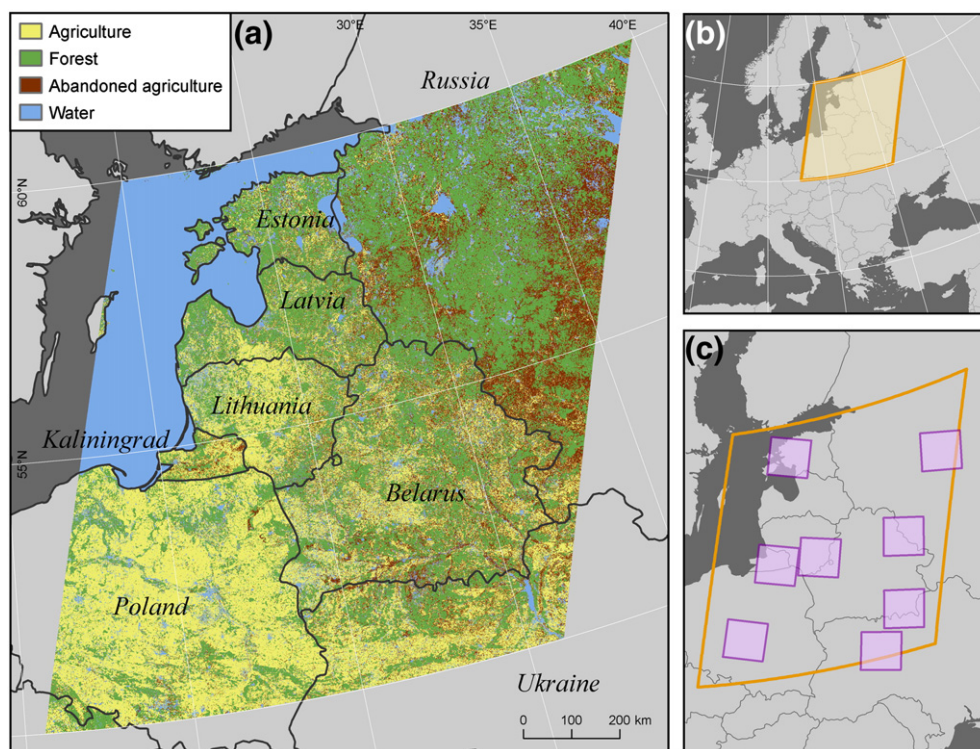


Fig. 2. Map of the study area in Eastern Europe. a) The most accurate MODIS classification based on growing period MODIS NDVI data for 2005 plus all phenology metrics obtained from MODIS NDVI from 2003 to 2008; b) Location of the study area within Europe (in orange); and c) Landsat footprints from where we selected training and validation data (in purple). (For interpretation of the references to color in this figure legend, the reader is referred to the web version of this article.)

agriculture we calculated eleven phenology metrics for each year. Phenology metrics are descriptive data of the growing period, calculated from fitted functions for each year of the NDVI time-series. The use of a fitting function smooths the data, thereby reducing noise and ensuring data consistency. We used the program TIMESAT to smooth the raw NDVI time series data and to calculate eleven phenology metrics for each year of the time series (Jonsson & Eklundh, 2004):

1. Start of the growing period: week of the year at which the left edge of the fitting function increased to 20% of the full amplitude of the growing period (i.e., the difference between the minimum NDVI, starting from the beginning of the year and the largest NDVI value of the fitting function);
2. End of the growing period: week of the year at which the right edge of the fitting function decreased to 20% of the amplitude of the growing period;
3. Length of the growing period: time in weeks between the start and the end of the growing period;
4. Base level: mean of minimum NDVI values before the start and after the end of the growing period;
5. Middle of the growing period: the mean (week) of the two weeks year at which the left edge of the fitted function has increased to the 80% level, and the right edge has decreased to the 80% level;
6. Maximum NDVI value for the fitted function during the growing period;
7. Amplitude of the growing period: difference between the base level NDVI value and the largest NDVI values of the fitted function (in NDVI values);
8. Rate of increase at the beginning of the growing period: ratio of the difference between the left 20% and 80% levels and the corresponding time difference in weeks (in NDVI values/Time (weeks));
9. Rate of decrease at the end of the growing period: Absolute value of the ratio of the difference between the right 20% and 80% levels and the corresponding time difference in weeks (in NDVI values/Time (weeks));
10. Large growing period integral: the area under the curve of the fitting function from the start to the end of the growing period;
11. Small growing period integral: the area under the curve of the fitting function between the start and the end of the growing period starting from the base level of the growing period.

NDVI values in the fitted function ranged from -3000 to $10,000$ with a scale factor of 0.00001 . We defined the growing period as starting on day 129 (May 9th, or May 8th on leap years) and ending on day 297 (October 24th, or October 23rd in leap years) based on initial TIMESAT results.

2.3. Training data for the classifications

Training data were extracted from land-cover maps that had been previously derived for three Landsat scenes: 186/022, 188/022 and 182/025 path/row (Worldwide Reference System, version 2) (Fig. 2c). Two of the Landsat land-cover classifications mapped land abandonment between 1989 and 1999 in parts of Lithuania and Russia. The overall accuracy was 92.6% for the classification of Landsat scene 186/022 (path/row) and 84.1% for the classification of 188/022 and between 80% and 91% accuracy for abandoned agriculture (Prishchepov et al., in review). The third Landsat scene was 182/025 and mapped abandonment between 1986 and 2000 around Chernobyl, Ukraine with an overall accuracy of 80.43% and 50% for agricultural abandonment (Hostert et al., 2011). The classification scheme included eight classes (Abandonment, Cropland, Grassland, Deciduous Forest, Needle-leaved Forest, Regrowth, Water, and Other Classes). Unfortunately, the dates of these two Landsat classifications

did not match the MODIS data record exactly, but these were the classifications that were closest to the MODIS data in time, and classifying additional Landsat images as input for MODIS classifications was beyond the scope of our study.

We summarized the percentage of each land-cover class in grid cells within 500-m resolution. The 500-m cells fully encompassed one 250-m pixel, leaving 125 m around the edges to account for location uncertainty in the MODIS VI data (Tan et al., 2006). For training purposes, we used 1459 cells with at least 90% dominance in one land-cover class. Training data was grouped into four classes: abandoned (157 cells), agriculture (444, both plowed fields and managed grasslands), forest (307, including deciduous, coniferous and mixed), and other (551, including water, urban, and wetlands) (Fig. 2c).

2.4. Classification algorithm, and classification tests

All land-cover classes exhibited multi-modal or non-normal reflectance distributions in our training data. In the case of abandoned agriculture, for example, areas covered by grasses versus young trees resulted in multi-modal distributions. We thus applied a non-parametric classifier, support vector machines (SVM) (Huang, Davis, & Townshend, 2002), to classify the MODIS data, since SVM do not require normally distributed training data.

SVM are a supervised computer learning method that can analyze and classify high-dimensional datasets. SVM employ non-parametric optimization algorithms to locate optimal boundaries between classes. SVM are superior to traditional classifiers and equivalent to other learning methods such as neural networks and decision trees (Huang et al., 2002). The principle behind SVM is called structural risk minimization (SRM). The risk of a learning machine (R) is bounded by the sum of empirical risk estimated from training samples (R_{emp}) and a confidence interval (Ψ):

$$R \leq R_{emp} + \Psi.$$

An SRM keeps the empirical risk (R_{emp}) constant and minimizes the confidence interval (Ψ), or maximizes the margin between a separating hyperplane and the closest data points. SVM fit an optimal separating hyperplane for each two classes of the training data in a multi-dimensional feature space. Boundaries are optimized to exclude outliers by minimizing errors among all possible boundaries separating the classes and minimizing confusion between classes. For linearly not separable classes, the input data are mapped into a higher dimensional space using an algorithm based on Lagrange multipliers and a kernel function.

Using SVM requires defining both a parameter for the kernel function (g) to map the input data into the higher dimensional space, as well as a regularization parameter (C) that is needed during the fitting of the hyperplane to the training data. The C parameter limits the influence of the training samples, whereas the kernel parameter g is a lower bound on the fraction of support vectors and an upper bound on the fraction of margin errors. The kernel parameter g defines the width of the Gaussian kernel function (or radial basis function, RBF), which implicitly transforms the classification problem into an infinite feature space. The Gaussian kernel is a so-called universal kernel, and a SVM with Gaussian kernel function can separate any class distribution at any precision. Once these parameters have been defined, the quadratic optimization applied during the training will always find the optimal solution and results are fully reproducible.

SVM are a binary classifier, i.e., they always separate two classes only. The strategy that we selected to conduct our MODIS classifications was the one-against-all strategy (OAA), where a set of binary classifiers is trained to separate each class from the rest; the maximum decision value determines the final class label.

The software package that we used was ImageSVM, programmed in IDL (Janz, van der Linden, Waske, & Hostert, 2007). SVMs are powerful classifiers, but different input time-series can result in different classifications accuracies. We therefore conducted 22 classifications and evaluated 10 questions to assess which subset of input from our pool of weekly red and near infrared MODIS time-series, weekly NDVI time-series, and annual phenology metrics resulted in the most reliable classification of abandoned agriculture (Table 1). These questions were:

1. Are near-infrared and red reflectance time-series better suited than NDVI time-series to map abandoned agriculture? This test was conducted with single-year time-series for the growing period only for both 2005 and 2006. We derived two classifications per year (one with red and near infrared time-series as input, one with NDVI time-series).
2. Do specific single-year growing period NDVI time-series provide better classification results than others? We classified growing period only NDVI time-series for each single year from 2003 to 2008.
3. Do time-series from the full year result in better classifications than time-series from the growing period only? We conducted four classifications for the year 2006: two using red and near-infrared reflectance time-series (one using all 46 images for the whole year, and one with 22 images for the growing period only) and two using NDVI time-series (one using 46 images and one with 22 images).
4. Does classification accuracy increase when using time-series from multiple years compared to single-year time-series? We conducted six classifications with growing period NDVI time-series: the first three were with single-year classifications for 2004, 2005 and 2006 respectively, the fourth used time-series for 2005 and 2006, the fifth used time-series for 2004 and 2006, and the sixth used time-series from all three years.
5. Do phenology metrics result in higher classification accuracies than NDVI time-series to map abandoned agriculture? We conducted seven classifications: the first classification was based on the eleven phenology parameters calculated for the full 2003–2008 NDVI time-series. Classifications two to seven included phenology parameters from a single year of growing period NDVI time-series for 2003, 2004, 2005, 2006, 2007, and 2008 respectively.
6. Do phenology metrics result in higher classification accuracies when used in conjunction with single-year growing period NDVI time-series? We conducted four classifications: classifications one and two included single-year growing period NDVI time-series for 2005 and 2006 respectively. Classifications three and four included the eleven phenology metrics calculated on the full (2003–2008) time series and single-year growing period NDVI time-series for 2005 and 2006, respectively.
7. Do phenology metrics from a time series of six years result in higher classification accuracies than phenology metrics from a time series of three years? We conducted four classifications: classifications one and two included the eleven phenology metrics from the full (6-year, 2003–2008) time series of NDVI data as well as single-year growing period NDVI time-series for 2005 and 2006, respectively. Classifications three and four included the same eleven phenology metrics calculated for a three-year (2004–2006) time series as well as single-year growing period NDVI time-series for 2005 and 2006, respectively.
8. Do phenology metrics based on the full time-series result in higher classification accuracies than phenology metrics based on single-year time-series? We conducted four classifications: classifications one and two included the phenology metrics from the full time series (2003–2008) as well as single-year growing period NDVI time-series for 2005 and 2006, respectively. Classifications three and four included phenology metrics based on the full time-series but single year period phenology metrics from 2005 and 2006 respectively plus their single-year growing period NDVI time-series for 2005 and 2006, respectively.
9. Are all eleven phenology metrics necessary or does it suffice to use a subset of the phenology metrics? We conducted two classifications: classification one included all eleven phenology metrics calculated from the 2004–2006 NDVI time series, as well as single-year growing period data for 2005. Classification two included only six phenology parameters (End of the growing period, start of the growing period, base level, maximum level, length of the growing period and middle of the growing period), with everything else equal to classification one.

Table 1

Conducted classifications, datasets included on each classification and comparisons made to find a suitable subset to map abandoned agriculture. The “x” in the “Included years” columns indicate the date or dates of the time-series included in the classification; the “X” indicates that both, the NDVI time-series and the Phenology metrics for that year, were included in the classification. The “x” in the “Addressed question” columns indicates the classification or classifications that were included to address each question.

Dataset	Bands	Included years						Addressed question										Coded name
		2003	2004	2005	2006	2007	2008	1	2	3	4	5	6	7	8	9	10	
NDVI (one year, growing period)	22	x							x		x							NDVI2003
NDVI (one year, growing period)	22		x							x	x	x						NDVI2004
NDVI (one year, growing period)	22			x					x	x	x	x	x					NDVI2005
NDVI (one year, growing period)	22				x				x	x	x	x	x	x				NDVI2006
NDVI (one year, growing period)	22					x				x		x						NDVI2007
NDVI (one year, growing period)	22						x		x			x						NDVI2008
NDVI (two years, growing period)	44		x	x								x						NDVI20042005
NDVI (two years, growing period)	44		x		x							x						NDVI20042006
NDVI (three years, growing period)	66		x	x	x							x						NDVI200420052006
NDVI (one full year)	46				x						x							NDVI2006all
Red and near infrared (one year, growing period)	44			x					x									REDNIR2005
Red and near infrared (one year, growing period)	44				x				x		x							REDNIR2006
Red and near infrared (one year, full year)	92				x						x							REDNIR2006all
Phenology (11 metrics, 6 years)	66	x	x	x	x	x	x					x						Ph0308
NDVI (one year, growing period) + phenology (11 metrics, 6 years)	88	x	x	x	X	x	x						x	x	x			NDVI2006ph0308
NDVI (one year, growing period) + phenology (11 metrics, 6 years)	88	x	x	X	x	x	x						x	x	x			NDVI2005ph0308
NDVI (one year, growing period) + phenology (11 metrics, 3 years)	55		x	x	X								x					NDVI2006ph0406
NDVI (one year, growing period) + phenology (11 metrics, 3 years)	55		x	X	x									x		x		NDVI2005ph0406
NDVI (one year, growing period) + phenology (11 metrics, 1 year)	33			X											x			NDVI2005ph0308_05
NDVI (one year, growing period) + phenology (11 metrics, 1 year)	33				X										x			NDVI2006ph0308_06
NDVI (one year, growing period) + phenology (6 metrics, 3 years)	40		x	X	x											x	x	NDVI2005ph0406S
NDVI (one year, 5 selected dates) + phenology (6 metrics, 1 year)	11				x												x	SNDVI05ph0406S_05

10. Are NDVI time-series from the entire growing period necessary or do NDVI images from a few dates within one year result in similar classification accuracies? We conducted two classifications: one classification included phenology metrics from the 2004–2006 NDVI time series, as well as the 2005 growing period NDVI time-series, and the second classification included the same phenology metrics, but only five selected NDVI images (first week of March, April, June, August, and October respectively).

2.5. Validation data

Independent validation data were collected for a stratified random sample in five Landsat footprints within the study area (Fig. 2c). Two Landsat images for each footprint were obtained from United States Geological Survey (USGS; <http://glovis.usgs.gov>), the first for the late 1980s and the second for either 2005 or 2006. To select pixels for validation, we used a grid of MODIS pixels with 2500-m distance between pixels to minimize spatial autocorrelation. Using the 2005 MODIS land-cover classification for stratification we selected 99 MODIS pixels for each of the four land-cover classes. The resultant MODIS pixels were interpreted visually using both Landsat images and, where available, high-resolution QuickBird images in GoogleEarth™. We recorded the dominant land-cover class for each pixel in 2005/06 and, in the case of abandoned agriculture, if the pixel was actively farmed in the late 1980s.

We generated an area-adjusted confusion matrix (Card, 1982; Stehman, 1996) for each classification and calculated the overall accuracy expressed by the kappa coefficient of agreement, the proportion of pixels correctly allocated, and the user's and producer's accuracy for each class.

Comparing classifications based on their kappa coefficient alone is not recommended, and statistical tests are necessary to properly judge if differences in classification accuracy are significant (Foody, 2004). We used McNemar tests to evaluate the statistical significance of the observed differences in the classification accuracies (De Leeuw et al., 2006; Foody, 2004). These tests are designed to evaluate differences among proportions that are not independent and have been widely used in remote sensing (Foody, 2009). The McNemar tests allowed us to compare all pair-wise combinations of any two maps using the same validation dataset. We calculated z-scores to allow testing if two classifications were significantly different at $\alpha = 0.05$ if $z = |1$. The z-score was calculated by normalizing the differences in the off diagonal of the cross-tabulation by:

$$z = \frac{V_{10} - V_{01}}{V_{10} + V_{01}}$$

Based on the statistical significance of the differences among the 22 classifications, we derived a hierarchical clustering distance dendrogram for each of the above questions.

3. Results

The best classification resulted from the growing period data for 2005 plus all phenology metrics from 2003 to 2008, with an overall area-adjusted accuracy of 69% (Interval 62.1–75.2), and for the abandoned agriculture class the lowest omission and commission area-adjusted errors (57.2% and 59.1% respectively), and the best producer's (42.7%) and user's (40.9%) area-adjusted accuracy. Based on this classification the land-cover class distribution was 29.6% agriculture (65.4% of producer's and 84.4% of user's area-adjusted accuracy), 33.8% forest (77.2% of producer's and 71.7% of user's area-adjusted accuracy), 15.1% abandoned agriculture, and 21.5% other land covers (85.1 of producer's and 63.2 of user's area-adjusted accuracy) (Table 2).

3.1. Classification tests

In terms of the 22 tested input datasets, the differences in the resulting classifications were small in most cases. Opposite but inconclusive results were found when comparing red and near-infrared reflectance data versus NDVI data. We compared two different years (2005 and 2006). For the year 2005, NDVI data performed better than red and near-infrared reflectance data (Fig. 3 Q1). When we compared classification accuracies for single years, all classifications for different years based on the growing period NDVI data resulted in kappa values over 61%, except 2004. The best classifications resulted from years 2003, 2005 and 2008 with overall accuracies over 62%; the years 2006 and 2007 resulted in classifications of slightly over 61% accuracy, and only 2004 resulted in a classification with overall accuracy slightly over 59% (Fig. 3 Q2). For the 2006, NDVI data resulted in slightly lower kappa values compared to the red and near-infrared reflectance data (Fig. 3 Q1), but the difference between NDVI and reflectance data-based classification accuracies was minor (Table 3).

Based on their McNemar scores, we found that classifications for single years from 2005 to 2008 were not significantly different from each other, but there were weak differences between all classifications and 2004 (Table 3, Fig. 4). Comparison between data for the entire year (2006) versus data for the growing period showed also only minor differences (Table 3, Fig. 3 Q3). Kappa values for the growing period were slightly higher for both red and near-infrared reflectance data and NDVI data (Fig. 3), but they were not significantly different from each other (Table 3). Classifications for 2005 were part of the same McNemar cluster (i.e., they were statistically not significantly different in terms of their accuracy, Fig. 4, cluster 4) whereas classifications for 2006 were part of a different McNemar cluster (Fig. 4, cluster 2).

When we compared classification accuracies for the entire growing period (2005) versus data for five selected dates in 2005 we found no significant differences. Kappa values for the five selected dates' classification showed slightly lower kappa values than the classification for the growing period and both classifications were part of the same McNemar cluster (Fig. 3 Q10).

Table 2

Error matrix of the classification with the best kappa error (NDVI for 2005, plus phenology data for 2003–2008). In bold font and located in the major diagonal of the error matrix are the number of sampled units correctly classified. Total sampled units for each class are highlighted in bold – italicized; in the columns the reference data are represented and in the rows the classification categories generated by the remotely sensed data.

		Area (km ²)	Reference				
			Agriculture	Forest	Abandoned Ag.	Other classes	Total
Classification	Agriculture	365,820	103	7	8	4	122
	Forest	417,750	12	81	18	2	113
	Abandoned agriculture	186,890	32	18	38	5	93
	Other classes	265,970	14	8	3	43	68
	Total	1,236,430	161	114	67	54	396

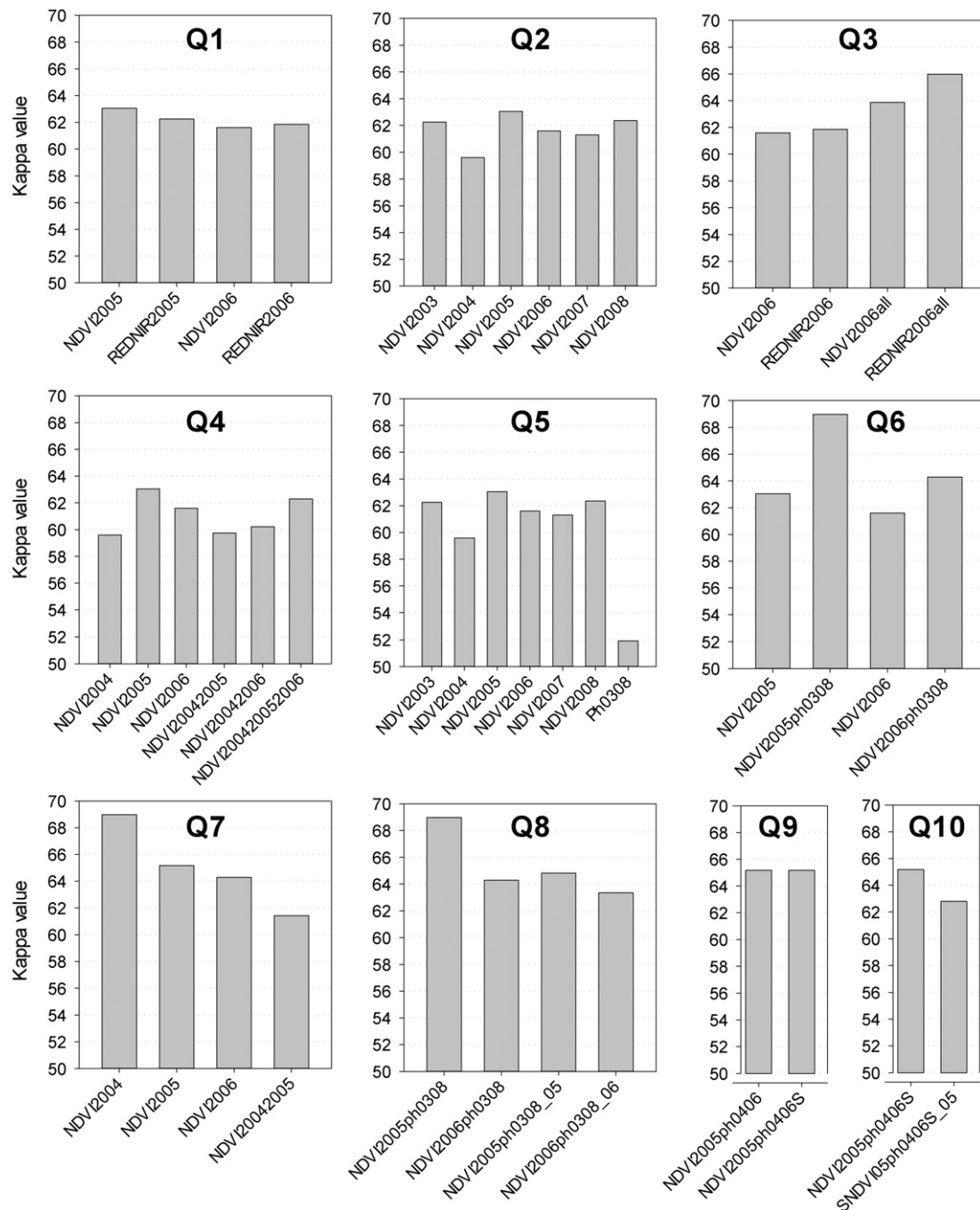


Fig. 3. Classification accuracies (Kappa values) for the classifications resulting from the different time-series. The charts represent our 10 questions to show which input data resulted in higher accuracies when mapping agricultural abandonment. Q1. NDVI versus red near-infrared; Q2. Individual years; Q3 Growing-season-only versus entire-year data. Q4 Multiple years; Q5. Phenology metrics versus NDVI time-series. Q6 Phenology metrics and NDVI time-series. Q7 NDVI time-series for six years versus time-series for three years. Q8. The full time series of phenology metrics versus phenology metrics time-series for single years. Q9 Eleven phenology metrics versus six phenology metrics. Q10 Growing period time-series versus selected NDVI dates. The name of each classification consists of five components: (1) type of input data, either normalized difference vegetation index (NDVI), phenology metrics (ph), or red and near-infrared reflectance data (REDNIR); (2) the year(s) of the input data (from 2003 to 2008); (3) whether the whole year (all) or only data from the growing period (without the "all" suffix) were considered; (4) whether only one year of phenology metrics, either 2005 (_05), 2006 (_06) was used or only a subset of 5 out of 11 phenology metrics (sel) was used; and (5) The inclusion of only 5 selected NDVI dates for first week of March, April, June, August, and October (the prefix S).

When we combined 2005 and 2004 growing period NDVI time-series, the classification accuracy stayed the same, but the use of 2004 plus 2006 time-series improved the classification. Similarly, the use of three years' time-series, from 2004 to 2006, did improve classification accuracy compared to the use of only two years of data (Fig. 3 Q4), but differences were not significant (Table 3). All classifications involving multiple years were part of the same McNemar cluster (Fig. 4, cluster 4).

Our tests of phenology metrics data showed the worst classification accuracies when we classified the phenology metrics alone (Fig. 3 Q5). However, combining phenology metrics with multiple-year NDVI data for the growing period did improve the classifications substantially (Fig. 3 Q6). Classifications that included both NDVI data and phenology metrics yielded five out of the six best classifications. The best performing out of all the 21 classifications conducted included all the phenology metrics from 2003 to 2008 plus the NDVI data for

Table 3
Significance of the differences in accuracies among our 22 MODIS classifications. Results are organized by McNemar significance test. There is no significant difference within each hierarchical cluster (McNemar).

Cluster group	1	2										3	4									
Classifications	NDVI2005ph0308	REDNIR2006all	NDVI2006all	REDNIR2006	NDVI2008	NDVI2006	SNDVI05ph0406S_05	NDVI2005ph0308_05	NDVI2006ph0308	NDVI2006ph0308_06	NDVI2005ph0406sel	NDVI2005ph0406	Ph0308	NDVI2003	NDVI2006ph0406	REDNIR2005	NDVI2007	NDVI2004	NDVI200420052006	NDVI2005	NDVI20042005	NDVI20042006
NDVI2005ph0308		**	**	**	**	**	**	*	*	*	*	*	****	***	*	***	***	***	***	***	***	***
REDNIR2006all													****				***	**	*	***	*	
NDVI2006all	**												***				**			*		
REDNIR2006	**												***				*					
NDVI2008	**												***				*					
NDVI2006	**												***				*					
SNDVI05ph0406S_05	**												***				**					
NDVI2005ph0308_05	**												****				**	*	*	**	*	
NDVI2006ph0308	*												****				**	*		**	**	
NDVI2006ph0308_06	*												***				**			*	*	
NDVI2005ph0406sel	**												***				**	*	**	**	*	
NDVI2005ph0406	**												***				**	*	**	**	*	
Ph0308	****	****	**	**	**	**	**	****	****	**	**	**		**	**	**	**		*	*		*
NDVI2003	***												**									
NDVI2006ph0406	**												**									
REDNIR2005	***												**									
NDVI2007	***												**									
NDVI2004	****	***	**	*	*	*	**	**	**	**	**	**										
NDVI200420052006	****	**					*	*		*	*	*	*									
NDVI2005	****	**					*			**	**	**	*									
NDVI20042005	****	***	*				**	**	*	**	**	**										
NDVI20042006	****	**					*	**	*	*	*	*	*									

2005 (Fig. 3 Q7). However, classifications that included phenology metrics for only one year based on a time series from 2003 to 2008 did not improve the performance of the classifier significantly (Fig. 3 Q8). Similarly, the inclusion of phenology metrics based on data from 2004 to 2006 resulted only in a minor improvement. Last but not least, the inclusion of all eleven phenology metrics versus the use of only five parameters made very little difference, and resulted in almost identical maps (Table 3, Fig. 3 Q9).

3.2. Mapping abandoned agriculture

In terms of the spatial patterns of the land-cover classes, all eight countries that were fully or partially included in our study area

exhibited abandoned agriculture (Fig. 5). The parts of Russia and Belarus that we mapped had the largest shares of abandoned agriculture of all the countries with 27.6% and 20.8% of their land area respectively. Three countries had 10–20% of abandoned agriculture (Ukraine (16.9%), Latvia (12.4%), and Estonia (11.7%)), and three countries had less than 10% (Lithuania (9.5%), Czech Republic (4.6%), and Poland (4.0%)) (Fig. 5).

In terms of forest, four countries had around 50% of their land covered by forest (Estonia (52.6%), Latvia (52%), and the portions mapped of Russia (51.4%) and Czech Republic (49.4%)). Three countries had around 30% of the land covered by forest (Belarus (36.3%), Lithuania (31.5%), and Ukraine (29%)). In contrast, Poland had only 21.3% of the land covered by forest (Fig. 5).

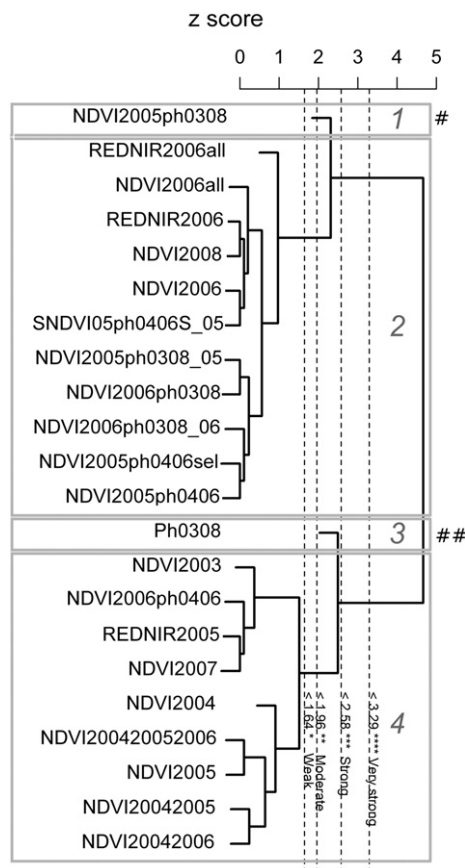


Fig. 4. Hierarchical clustering of the classifications resulting from the different sets of input data using McNemar test values as the distance metric. The best classification is marked with a # and the worst classification is marked with a ##. Clusters represent classifications that were statistically more similar and are indicated by gray lines that separate the McNemar Cluster Groups. Dotted lines represent the threshold at which there is a significant difference at a p-value of >0.10: *, >0.05–0.10: **, >0.01–0.05: ***, >0.001–0.01: ****. The name of each classification has five components: 1) type of input data, either normalized difference vegetation index (NDVI), phenology metrics (ph), or red and near-infrared reflectance data (REDNIR); 2) the year or years of the input data (from 2003 to 2008); 3) the inclusion of the entire year (all); or data only for the growing period (classification names without the “all” suffix); 4) the classifications with only one year of phenology metrics, either 2005 (_05), 2006 (_06) or only a subset of 5 out of 11 phenology metrics (sel); and 5) the inclusion of only 5 selected NDVI dates for first week of March, April, June, August, and October (the prefix S) respectively.

In terms of the relative areas mapped as agriculture, Poland had the most (66.8%) followed by Lithuania, Ukraine, Czech Republic, and Belarus (48.3%, 45.5%, 38.6% and 32.1% respectively). Latvia and Estonia were the countries with the least agriculture (24.4% and 18.0% respectively).

3.3. Validation

According to our validation data, 51 out of 67 of sampling points (76.12%) that we classified as abandoned agriculture from the MODIS imagery from 2005/06 were indeed farmed in the late 1980s and in an early successional stage by 2005/06. Only 16 sampling points out of the 67 (23.88%) were not agriculture in the late 1980s, but already covered by shrubs then. These may represent either permanent shrublands or pre-1980s abandoned agriculture, but we could not assess which of these two were more common.

All classifications had kappa values above 51% (Fig. 3). Using the McNemar test as distance metric for a hierarchical clustering, we found four significantly different clusters of classifications (Fig. 4, Table 3). The best performing classification was in cluster one, which included only one classification (2005 NDVI growing period data plus phenology metrics from 2003 to 2008). Cluster two

included eleven classifications with intermediate results, subdivided into two subgroups: one with four classifications based on data from 2006, a classification based on data from 5 selected 2005 NDVI dates and 2005 phenology metrics from 2004 to 2006 and one with NDVI data from 2008. The second subgroup had five classifications and all of the classifications in the second group of cluster two included phenology metrics (Table 1, Fig. 4). The classification with best performance for cluster two included red and near infrared 2006 data for the whole year (Kappa value of 66%).

Cluster three, with one map, had the worst accuracy. This classification included only phenology metrics from 2003 to 2008 (Table 1, Fig. 4). Cluster four was composed by nine classifications with kappa values from 59.8 to 63.1% (Figs. 3 and 4). Cluster four included four classifications based on growing period NDVI data for one year (years 2003, 2004, 2005, and 2007), and three classifications that included NDVI data for two and three years (2004, 2005, 2006 and the combinations among them). In comparison with the nine classifications included in cluster four, the classification for 2005 NDVI growing period data had slightly better results, followed by the growing period NDVI data for 2003 and then growing period NDVI data for years 2004–2006. The last two classifications in cluster four utilized either red and near-infrared reflectance data for the 2005 growing period, or NDVI data for 2006 plus phenology metrics based on data from 2004 to 2006 (Table 1, Fig. 4).

4. Discussion

Our results showed that it is possible to map abandoned agriculture for large areas using MODIS 250-m data with overall accuracies of about 65%. This result was similar to the accuracies reported for other equally complex MODIS-based land-cover classifications (Clark, Aide, Grau, & Riner, 2010; Jin & Sader, 2005; Spruce et al., 2011). Abandoned agriculture was widespread in our study area, covering approximately 15% of the land. When comparing this number to the remaining 30% of land in agriculture, we deduce that about 45% of the area was farmed in the 1980s and a third of those areas were abandoned. Our validation data showed that a clear majority (> 75%) of the areas mapped as abandoned agriculture were indeed actively farmed during the 1980s, highlighting how rapid the abandonment process was in the first two decades after the collapse of the USSR.

Classification errors of the abandoned agriculture class largely occurred due to confusion with the agriculture class. This was likely due to two reasons. The first reason is spatial proximity; many abandoned agriculture areas were intermixed with still active agriculture. During socialism, the decision which crops to plant was made for large areas and in 5-year plans for entire regions. After the collapse of the USSR, landownership became more fragmented, the decision whether to continue cultivation or not was made individually, and fields were often much smaller than in socialist times. The second reason for classification errors are the MODIS gridding artifacts that cause changes in the spectral information reported for a given MODIS pixel over time (Tan et al., 2006). The inherent limitations of the MODIS data thus make it difficult to map abandoned agriculture, but our results are encouraging. Based on our results, we suggest that mapping abandoned agriculture is challenging but the use of MODIS a valid option when mapping at regional to global scales. Mapping abandoned agriculture regularly with MODIS could highlight areas of rapid change, and suggest where to conduct more detailed classifications with finer-resolution satellite data.

It was also encouraging to see that the rates of abandonment that we found were in close agreement with more localized studies that have used Landsat images to map abandoned agriculture and also with statistical data. In Russia, the reported declines of arable land based on official statistics reached 20% due to the transition to a market economy (Ioffe & Nefedova, 2004). Of the 127 million ha of farmland in the early 1980s, 20 to 30 million were no longer used by the

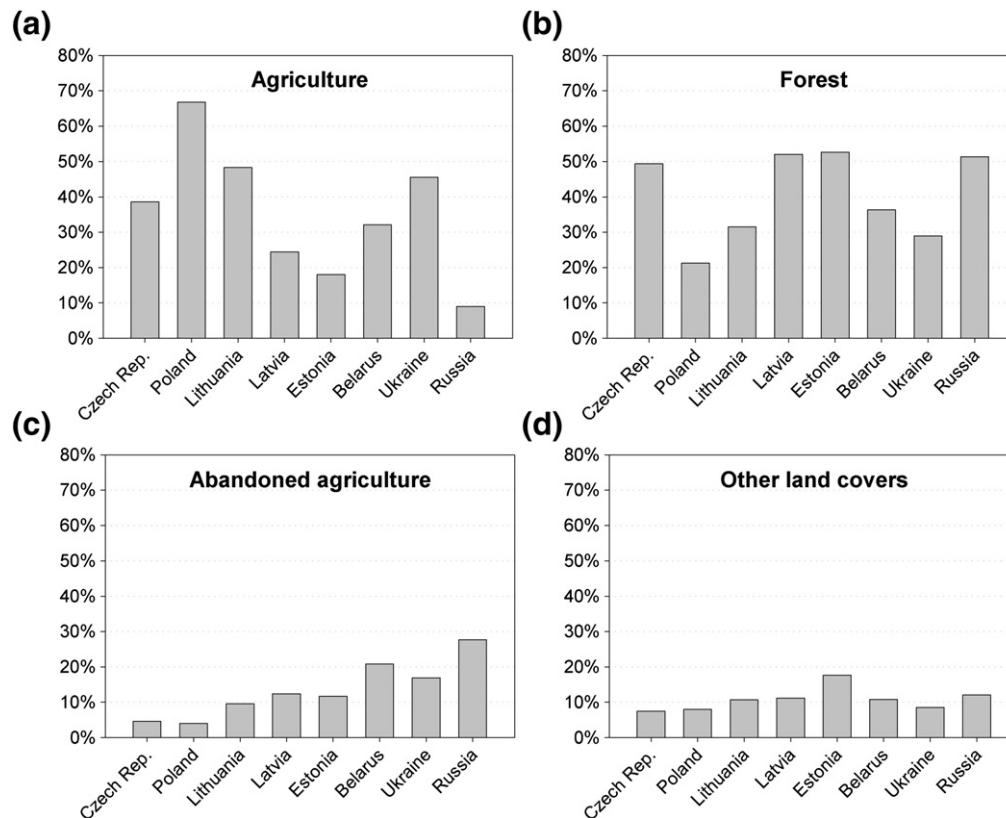


Fig. 5. Land-cover class distributions for each country based on the best classification, which resulted from the growing-season MODIS NDVI data for 2005 plus all phenology parameters obtained from MODIS NDVI data from 2003 to 2008.

early 2000s (Franks & Davydova, 2005; Ioffe, Nefedova, & Zaslavsky, 2004; Ioffe, 2005). Similarly, the Landsat based classifications of abandonment covering 5% of our study area (see above) had 37.5% agriculture, 33.4% forest, and 18% abandonment respectively (compared to 30% agriculture, 34% forest, 15% abandoned agriculture, and 21% other land cover that we found for the entire MODIS tile).

We conducted numerous comparisons to identify the optimal input data for mapping abandoned agriculture and these comparisons provided interesting results. The use of near-infrared and red reflectance data instead of NDVI data did not improve the classification accuracy significantly according to the McNemar tests. In other words, NDVI data captured the information necessary to classify abandoned agriculture as well as the near-infrared and red reflectance data. Since there was no significant difference in the classifications obtained from NDVI and near-infrared and red reflectance data, we recommend the use of NDVI data to classify abandoned agriculture, reducing the data volume by 50%.

We also did not find that a certain year resulted in significantly more accurate classifications of abandoned agriculture. The early years (2003–2004) had lower accuracies, but that may be due to later dates of our training and validation data. The fact that there was not a clear best year to map abandoned agriculture was encouraging, and suggests that the best quality data that is closest in time to the training and validation datasets will provide the best results. In our case the best year was 2005.

The use of data for the entire year instead of growing-period-only data also did not make a significant difference in our results. Entire-year data resulted in better overall accuracies than growing-period-only data, but this finding was not statistically significant. We recommend the use of growing-period data to conduct classifications on abandoned agriculture reducing the data volume to 22 images for a growing period instead of the 46 for the whole year.

The inclusion of a second year of MODIS data did improve classification accuracies, and it did matter if the two years were contiguous. We recommend the inclusion of at least two years of NDVI data close to the dates of the validation and training data to conduct classifications on abandoned agriculture. If only two years are included, we recommend including two years that are not immediately subsequent (in our case 2004 and 2006), which can help to avoid falsely classifying temporarily fallow fields as abandoned.

The use of phenology metrics alone resulted in our worst classification, but coupled with NDVI growing period data, the phenology metrics resulted in our best classification (i.e., for 2005 growing-period data plus phenology metrics). We thus recommend the inclusion of phenology metrics when mapping abandoned agriculture. Six phenology metrics captured the information necessary to classify abandoned agriculture just as well as all eleven phenology metrics. This is why we recommend the use of only six metrics (End of the growing period, start of the growing period, base level, maximum level, length of the growing period and middle of the growing period) coupled with NDVI data, reducing the data volume by 45%. The six phenology metrics that were most important also made biological sense. For instance, the start of the period was important because shrublands and forest green up earlier than agricultural areas, which typically green up after being plowed and sowed (in the case of summer crops). Equally important was the end of the growing period, because agricultural areas senesced earlier than other land-cover types, crops were harvested, and land was plowed and prepared for the next year. In contrast, shrubland areas exhibited a later end of the growing period. The maximum NDVI value during the growing period was important as well, since active agricultural areas showed higher values than all other classes. The length of the growing period was longest for forests and shorter for shrublands and abandoned agriculture. The middle of the growing period, as

calculated by TIMESAT, helped to discriminate abandoned agricultural land from actively used croplands since agriculture had an earlier growing period. Base level helped to discriminate other classes such as urban and water bodies from forest, shrublands, and agricultural abandoned land.

The limited number of statistically significant different classifications highlighted the importance of using the McNemar test when comparing multiple maps. Raw accuracies alone can be misleading because higher accuracies for one classification over another may not be statistically significant. Hierarchical cluster dendrograms offer an easy way to visualize multiple McNemar comparisons, which facilitate the analysis and selection of classifications to be used for other purposes.

In terms of the patterns of abandoned agriculture, our study area covered eight Eastern European countries either in parts, or in their entirety. Lithuania, Latvia, Estonia, and Belarus were entirely mapped and more than 75% of Poland was mapped, making it possible to compare them. In Poland, only a small amount of agriculture was abandoned after the collapse of the USSR. Abandoned agriculture areas were concentrated in protected areas in the north of the country, and in places in the South where economical activities shifted from agriculture to industry in the south. In Latvia and Estonia, abandoned agriculture was widespread, covering in 2005 about 39% of what was agriculture in the 1980s. Given similar historical processes for all three Baltic countries, it was somewhat surprising that Lithuania had less abandoned agriculture than Latvia and Estonia (only 16% of what was formerly agriculture was abandoned agriculture by 2005). However, both Latvia and Estonia had more forest than Lithuania. Also, economic growth patterns differed among the three countries; Lithuania had one of the fastest growing economies of the European Union, compared with Latvia which was one of the poorest economies of the European Union. Both Latvia and Estonia have also been hit hard by the economic crises that started in 2008–2009. Those economic differences may have resulted in less abandoned agriculture in Lithuania compared to Latvia and Estonia. In the case of Belarus, abandoned agriculture reached more than 39% of the areas that were agriculture in the 1980s. However Belarus' economy is still state-controlled, and industrial production plunged in the early 1990s because of decreases in imported inputs, in investment, and in demand for exports from traditional trading partners. Of all the countries, the part of Russia that we analyzed had the most abandoned agriculture: more than 75% of the areas that were used for agriculture in the 1980s were abandoned according to our analysis.

Our findings confirmed that abandoned agriculture is widespread in Eastern Europe, but abandonment is not unique to Eastern Europe. It is necessary to conduct similar studies worldwide to understand the pattern of abandoned agriculture, and its environmental, social, and food production trade-offs and opportunities. Land abandonment can be a consequence of socio-economic and environmental changes, as well as the results of new hazards, and technology. The reasons for land abandonment can range from changes in land tenure to the simple “recovery” that a landowner decides to give to a field to allow soils to replenish and nutrients to recover. The process of land abandonment can be abrupt, in which case the land is no longer used, or gradual, e.g., when grazing replaces the production of crops or fields are used only every second or third year. After abandonment, different successional pathways can occur depending on prior land uses, and the environmental conditions of the land.

Reductions in agricultural production can have negative social and economic implications, but they can also provide an opportunity for conservation and environmental protection (Young et al., 2005). Given the strong ramifications of agricultural abandonment, and the potential role of these lands to relax pressure from natural ecosystems elsewhere (Lambin & Meyfroidt, 2011a,b) mapping and monitoring abandoned farmland should be a top research priority. We identified approaches here to map abandoned agriculture at broad

scales, which is important given the paucity of reliable data on abandoned agriculture.

Acknowledgments

We gratefully acknowledge support by Consejo Nacional de Ciencia y Tecnología (CONACyT, Mexico), the NASA Land-Cover and Land-Use Change Program, the Einstein Foundation, the European Commission (VOLANTE, FP7-ENV-2010-265104), and the University of Wisconsin-Madison. Two anonymous reviewers provided helpful comments, which greatly improved the manuscript. P. Hostert and A. Sieber from Humboldt-University Berlin generously shared their classification of abandonment near Chernobyl. We also express our gratitude to University of Wisconsin-Madison SILVIS lab fellows, especially to M. Dubinin and M. Baumann, for their technical assistance and fruitful discussions.

References

- Aide, T. M., & Grau, H. R. (2004). Globalization, migration, and Latin American ecosystems. *Science*, 305(5692), 1915–1916.
- Aide, T. M., Zimmerman, J. K., Herrera, L., Rosari, M., & Serrano, M. (1995). Forest recovery in abandoned tropical pastures in Puerto Rico. *Forest Ecology and Management*, 77, 77–86.
- Baumann, M., Kuemmerle, T., Elbakidze, M., Ozdogan, M., Radeloff, V. C., Keuler, N. S., et al. (2011). Patterns and drivers of post-socialist farmland abandonment in Western Ukraine. *Land Use Policy*, 28, 552–562.
- Bergen, K. M., Zhao, T., Kharuk, V., Blam, Y., Brown, D. G., Peterson, L. K., et al. (2008). Changing regimes: Forested land-cover dynamics in central Siberia 1974–2001. *Photogrammetric Engineering and Remote Sensing*, 74, 787–798.
- Card, D. H. (1982). Using known map category marginal frequencies to improve estimates of thematic map accuracy. *Photogrammetric Engineering and Remote Sensing*, 48, 431–439.
- Charles, D. (2010). Renewing the post-Soviet steppe. *Science*, 328, 1225.
- Chauchard, S., Carcaillet, C., & Guibal, F. (2007). Patterns of land-use abandonment control tree-recruitment and forest dynamics in Mediterranean mountains. *Ecosystems*, 10, 936–948.
- Clark, M. L., Aide, T. M., Grau, H. R., & Riner, G. (2010). A scalable approach to mapping annual land cover at 250 m using MODIS time series data: A case study in the Dry Chaco ecoregion of South America. *Remote Sensing of Environment*, 114, 2816–2832.
- Cramer, V. A., Hobbs, R. J., & Standish, R. J. (2008). What's new about old fields? Land abandonment and ecosystem assembly. *Trends in Ecology & Evolution*, 23, 104–112.
- De Leeuw, J., Jia, H., Yang, L., Liu, X., Schmidt, K., & Skidmore, A. (2006). Comparing accuracy assessments to infer superiority of image classification methods. *International Journal of Remote Sensing*, 27, 223–232.
- Dutch National Reference Center for Agriculture, Nature and Food Quality, Latvian Ministry of Agriculture, & Latvian State (2005). Land abandonment and biodiversity, in relation to the 1st and 2nd pillars of the European Union's Common Agricultural Policy: Outcome of an international seminar in Sigulda, Latvia, 7–8 October 2004. *Pre-accession short programme of The Netherlands Ministry of Economic Affairs. Utrecht D.L.G.* (pp. 1–64).
- Egbert, S. L., Lee, R. Y., Price, K. P., & Boyce, R. (1998). Mapping Conservation Reserve Program grasslands using multi-seasonal thematic mapper imagery. *Geocarto International*, 13, 17–24.
- Egbert, S. L., Park, S., Price, K. P., Lee, R., Wu, J., & Duane Nellis, M. (2002). Using Conservation Reserve Program maps derived from satellite imagery to characterize landscape structure. *Computers and Electronics in Agriculture*, 37, 141–156.
- Ellis, E. C., Goldewijk, K. K., Siebert, S., Lightman, D., & Ramankutty, N. (2010). *Anthropogenic transformation of the biomes, 1700 to 2000*. geb. 540.
- Faluccci, A., Maiorano, L., & Boitani, L. (2007). Changes in land-use/land-cover patterns in Italy and their implications for biodiversity conservation. *Landscape Ecology*, 22, 617–631.
- Farley, K. A. (2007). Grasslands to tree plantations: Forest transition in the Andes of Ecuador. *Annals of the Association of American Geographers*, 97, 755–771.
- Fassnacht, K. S., Cohen, W. B., & Spies, T. A. (2006). Key issues in making and using satellite-based maps in ecology: A primer. *Forest Ecology and Management*, 222, 167–181.
- Fensholt, R., & Sandholt, I. (2005). Evaluation of MODIS and NOAA AVHRR vegetation indices with in situ measurements in a semi-arid environment. *International Journal of Remote Sensing*, 26, 2561–2594.
- Foley, J. A., DeFries, R. S., Asner, G. P., Barford, C., Bonan, G., Carpenter, S. R., et al. (2005). Global consequences of land use. *Science*, 309, 570–574.
- Foley, J. A., Ramankutty, N., Brauman, K. A., Cassidy, E. S., Gerber, J. S., Johnston, M., et al. (2011). Solutions for a cultivated planet. *Nature*, 478, 337–342. <http://dx.doi.org/10.1038/nature10452>.
- Food and Agriculture Organization of the United Nations (2010). FAOSTAT data web page. <http://faostat.fao.org/> Last viewed in May 13 2012
- Foody, G. M. (2004). Thematic map comparison: Evaluating the statistical significance of differences in classification accuracy. *Photogrammetric Engineering and Remote Sensing*, 70, 627–634.

- Foody, G. M. (2009). Sample size determination for image classification accuracy assessment and comparison. *International Journal of Remote Sensing*, 30, 5273–5291.
- Franks, J. R., & Davydova, I. (2005). Reforming the farming sector in Russia, new options for old problems. *Outlook on Agriculture*, 34, 97–103.
- Friedl, M. A., & Brodley, C. E. (1997). Decision tree classification of land cover from remotely sensed data. *Remote Sensing of Environment*, 61, 399–409.
- Friedl, M. A., McIver, D. K., Hodges, J. C. F., Zhang, X. Y., Muchoney, D., Strahler, A. H., et al. (2002). Global land-cover mapping from MODIS: Algorithms and early results. *Remote Sensing of Environment*, 83, 287–302.
- Goldewijk, K. K., & Ramankutty, N. (2004). Land-cover change over the last three centuries due to human activities: The availability of new global data sets. *Geojournal*, 61, 335–344.
- Goncalves, P., Carrão, H., Pinheiro, A., & Caetano, M. (2005). Land-cover classification with a support vector machine applied to MODIS imagery. *Proceedings of the 25th Annual Symposium of the European Association of Remote Sensing Laboratories, Porto, Portugal, June 6–11* (pp. 517–525).
- Grau, H. R., Aide, T. M., Zimmerman, J. K., Thomlinson, J. R., Helmer, E., & Zou, X. (2003). The ecological consequences of socioeconomic and land-use changes in postagricultural Puerto Rico. *BioScience*, 53, 1159–1168.
- Haberl, H., Erb, K. H., Krausmann, F., Gaube, V., Bondeau, A., Plutzar, C., et al. (2007). Quantifying and mapping the human appropriation of net primary production in earth's terrestrial ecosystems. *Proceedings of the National Academy of Sciences*, 104, 12942–12947.
- Hermes, L., Friauff, D., Puzicha, J., & Buhmann, J. M. (1999). Support vector machines for land usage classification in Landsat TM imagery. *Proc. IGARSS'99*, 1, (pp. 348–350).
- Herold, M., Mayaux, P., Woodcock, C. E., Baccini, A., & Schmullius, C. (2008). Some challenges in global land-cover mapping: An assessment of agreement and accuracy in existing 1 km datasets. *Remote Sensing of Environment*, 112, 2538–2556.
- Hostert, P., Kuemmerle, T., Prishchepov, A., Sieber, A., Lambin, E. F., & Radeloff, V. C. (2011). Rapid land use change after socio-economic disturbances: The collapse of the Soviet Union versus Chernobyl. *Environmental Research Letters*, 6, 045201.
- Huang, C., Davis, L. S., & Townshend, J. R. G. (2002). An assessment of support vector machines for land-cover classification. *International Journal of Remote Sensing*, 23, 725–749.
- Ioffe, G. (2005). The downsizing of Russian agriculture. *Europe-Asia Studies*, 57, 179–208.
- Ioffe, G., & Nefedova, T. (2004). Marginal farmland in European Russia. *Eurasian Geography and Economics*, 45, 45–59.
- Ioffe, G., Nefedova, T., & Zaslavsky, I. (2004). From spatial continuity to fragmentation: The case of Russian farming. *Annals of the Association of American Geographers*, 94, 913–943.
- Jacquin, A., Sheeren, D., & Lacombe, J. (2010). Vegetation cover degradation assessment in Madagascar savanna based on trend analysis of MODIS NDVI time series. *International Journal of Applied Earth Observation and Geoinformation*, 12, S3–S10.
- Janz, A., van der Linden, S., Waske, B., & Hostert, P. (2007). ImageSVM — A user-oriented tool for advanced classification of hyperspectral data using support vector machines. In I. Reusen, & J. Cools (Eds.), *Proc. 5th Workshop EARSeL SIG Imaging Spectroscopy*. Bruges, Belgium, 1, (pp. 1–5).
- Jin, S., & Sader, S. A. (2005). MODIS time-series imagery for forest disturbance detection and quantification of patch size effects. *Remote Sensing of Environment*, 99, 462–470.
- Jonsson, P., & Eklundh, L. (2004). TIMESAT — A program for analyzing time-series of satellite sensor data. *Computers & Geosciences*, 30, 833–845.
- Justice, C. O., Townshend, J. R. G., Fermote, V., Masuoka, E., Wolfe, R. E., Saleous, N., et al. (2002). An overview of MODIS Land data, processing and product status. *Remote Sensing of Environment*, 83, 3–15.
- Kauppi, P. E., Ausubel, J. H., Fang, J., Mather, A. S., Sedjo, R. A., & Waggoner, P. E. (2006). Returning forests analyzed with the forest identity. *Proceedings of the National Academy of Sciences*, 103, 17574–17579.
- Klooster, D. (2003). Forest transitions in Mexico: Institutions and forests in a globalized countryside. *The Professional Geographer*, 55, 227.
- Kristensen, L. S., Thenail, C., & Kristensen, S. P. (2004). Landscape changes in agrarian landscapes in the 1990s: The interaction between farmers and the farmed landscape. A case study from Jutland, Denmark. *Journal of Environmental Management*, 71, 231–244.
- Kuemmerle, T., Hostert, P., Radeloff, V. C., van der Linden, S., Perzanowski, K., & Kruhlov, I. (2008). Cross-border comparison of post-socialist farmland abandonment in the Carpathians. *Ecosystems*, 11, 614–628.
- Kuemmerle, T., Kozak, J., Radeloff, V. C., & Hostert, P. (2009). Differences in forest disturbance among land ownership types in Poland during and after socialism. *Journal of Land Use Science*, 4, 73–83.
- Lambin, E. F., & Geist, H. J. (Eds.). (2006). *Land-use and land-cover change: Local processes and global impacts* (pp. 222). Berlin Heidelberg New York: Springer.
- Lambin, E. F., & Meyfroidt, P. (2011a). Global land use change, economic globalization, and the looming land scarcity. *Proceedings of the National Academy of Sciences of the United States of America*, 108(9), 3465–3472. <http://dx.doi.org/10.1073/pnas.1100480108>.
- Lambin, E. F., & Meyfroidt, P. (2011b). Global land use change, economic globalization, and the looming land scarcity. *Proceedings of the National Academy of Sciences of the United States of America*, 108, 3465–3472.
- Leff, B., Ramankutty, N., & Foley, J. A. (2004). Geographic distribution of major crops across the world. *Global Biogeochemical Cycles*, 18, 1–27.
- Lepers, E., Lambin, E. F., Janetos, A. C., DeFries, R. S., Achard, F., Ramankutty, N., et al. (2005). A synthesis of information on rapid land-cover change for the period 1981–2000. *BioScience*, 55, 115–124.
- Lesschen, J., Cammeraat, L., Kooijman, A., & Van Wesemael, B. (2008). Development of spatial heterogeneity in vegetation and soil properties after land abandonment in a semi-arid ecosystem. *Journal of Arid Environments*, 72, 2082–2092.
- Lu, D., Mausel, E., Brondizios, E., & Moran, E. (2004). Change detection techniques. *International Journal of Remote Sensing*, 25, 2365–2407.
- MacDonald, D., Crabtree, J. R., Wiesinger, G., Dax, T., Stamou, N., Fleury, P., et al. (2000). Agricultural abandonment in mountain areas of Europe: Environmental consequences and policy response. *Journal of Environmental Management*, 59, 47–69.
- Meyfroidt, P., & Lambin, E. F. (2008). Forest transition in Vietnam and its environmental impacts. *Global Change Biology*, 14, 1319–1336.
- Millennium Ecosystem Assessment (2005). *Ecosystems and human well-being: Current state and trends: Findings of the Condition and Trends Working Group*. Washington DC: Island Press 917 pp.
- Moreira, F., & Russo, D. (2007). Modeling the impact of agricultural abandonment and wildfires on vertebrate diversity in Mediterranean Europe. *Landscape Ecology*, 22, 1461–1476.
- Müller, D., Kuemmerle, T., Rusu, M., & Griffiths, P. (2009). Lost in transition: Determinants of post-socialist cropland abandonment in Romania. *Journal of Land Use Science*, 4, 109–129.
- Nikodemus, O., Bell, S., Grine, I., & Liepins, I. (2005). The impact of economic, social and political factors on the landscape structure of the Vidzeme uplands in Latvia. *Landscape and Urban Planning*, 70, 57–67.
- Park, S., & Egbert, S. (2008). Remote sensing-measured impacts of the Conservation Reserve Program on landscape structure in southwestern Kansas. *GIScience & Remote Sensing*, 45, 83–108.
- Peterson, U., & Aunap, R. (1998). Changes in agricultural land use in Estonia in the 1990s detected with multitemporal Landsat MSS imagery. *Landscape and Urban Planning*, 41, 193–201.
- Poyatos, R., Latron, J., & Llorens, P. (2003). Land use and land-cover change after agricultural abandonment: The case of a Mediterranean mountain area (Catalan Pre-Pyrenees). *Mountain Research and Development*, 23, 362–368.
- Prishchepov, A., Radeloff, V. C., Dubinin, M., & Alcantara, C. (in review). The effect of image acquisition dates on detection of agricultural land abandonment in Eastern Europe. *Remote Sensing of Environment*.
- Ramankutty, N., & Foley, J. A. (1999). Estimating historical changes in global land cover: Croplands from 1700 to 1992. *Global Biogeochemical Cycles*, 13, 997–1027.
- Ramankutty, N., Gibbs, H. K., Achard, F., DeFries, R. S., Foley, J. A., & Houghton, R. A. (2007). Challenges to estimating carbon emissions from tropical deforestation. *Global Change Biology*, 13, 51–66.
- Ramankutty, N., Heller, E., & Rhemtulla, J. (2010). Prevailing myths about agricultural abandonment and forest regrowth in the United States. *Annals of the Association of American Geographers*, 100, 502–512.
- Redo, D., Joby Bass, J. O., & Millington, A. C. (2009). Forest dynamics and the importance of place in western Honduras. *Applied Geography*, 29, 91–110.
- Rey Benayas, J. M., Martins, A., Nicolau, J. M., & Schulz, J. J. (2007). Abandonment of agricultural land: An overview of drivers and consequences. *CAB Reviews: Perspectives in Agriculture, Veterinary Science, Nutrition and Natural Resources*, 2, 1–14.
- Romero-Calcerrada, R., & Perry, G. L. W. (2004). The role of land abandonment in landscape dynamics in the SPA Encinares del río Alberche y Cofio, Central Spain, 1984–1999. *Landscape and Urban Planning*, 66, 217–232.
- Rudel, T. K., Coomes, O. T., Moran, E., Achard, F., Angelsen, A., Xu, J., et al. (2005). Forest transitions: Towards a global understanding of land use change. *Global Environmental Change Part A*, 15, 23–31.
- Russo, D. (2007). The effects of land abandonment on animal species in Europe: Conservation and management implications. *Integrated assessment of vulnerable ecosystems under global change in the European Union. Directorate-General for Research Environment, European Commission* (pp. 1–53). Brussels, Luxembourg: Office for Official Publications of the European Communities.
- Sloan, S. (2008). Reforestation amidst deforestation: Simultaneity and succession. *Global Environmental Change*, 18, 425–441.
- Spruce, J. P., Sader, S., Ryan, R. E., Smoot, J., Kuper, P., Ross, K., et al. (2011). Assessment of MODIS NDVI time series data products for detecting forest defoliation by gypsy moth outbreaks. *Remote Sensing of Environment*, 115, 427–437.
- Stehman, S. (1996). Estimating the kappa coefficient and its variance under stratified random sampling. *Photogrammetric Engineering and Remote Sensing*, 62, 401–407.
- Stoate, C., Boatman, N. D., Borralho, R. J., Carvalho, C. R., Snoo, G. R. D., & Eden, P. (2001). Ecological impacts of arable intensification in Europe. *Journal of Environmental Management*, 63, 337–365.
- Tan, B., Woodcock, C. E., Hu, J., Zhang, P., Ozdogan, M., Huang, D., et al. (2006). The impact of gridding artifacts on the local spatial properties of MODIS data: Implications for validation, compositing, and band-to-band registration across resolutions. *Remote Sensing of Environment*, 105, 98–114.
- Tilman, D. (1999). Global environmental impacts of agricultural expansion: The need for sustainable and efficient practices. *Proceedings of the National Academy of Sciences of the United States of America*, 96, 5995–6000.
- Tilman, D., Fargione, J., Wolff, B., D'Antonio, C., Dobson, A., Howarth, R., et al. (2001). Forecasting agriculturally driven global environmental change. *Science*, 292, 281–284.
- Vandermeer, J., & Perfecto, I. (2007). The agricultural matrix and a future paradigm for conservation. *Conservation Biology*, 21, 274–277.
- White, M. A., de Beurs, K. M., Didan, K., Inouye, D. W., Richardson, A. D., Jensen, O. P., et al. (2008). Intercomparison, interpretation, and assessment of spring phenology in North America estimated from remote sensing for 1982 to 2006. *Remote Sensing of Environment*, 112, 4333–4343.
- Xiao, X., Hagen, S., Zhang, Q., Keller, M., & Moore, B. (2006). Detecting leaf phenology of seasonally moist tropical forests in South America with multi-temporal MODIS images. *Remote Sensing of Environment*, 103, 465–473.
- Yang, F., Ichii, K., White, M. A., Hashimoto, H., Michaelis, A. R., Votava, P., et al. (2007). Developing a continental-scale measure of gross primary production by combining

- MODIS and AmeriFlux data through support vector machine approach. *Remote Sensing of Environment*, 110, 109–122.
- Young, J., Watt, A., Nowicki, P., Alard, D., Clitherow, J., Henle, K., et al. (2005). Towards sustainable land use: Identifying and managing the conflicts between human activities and biodiversity conservation in Europe. *Biodiversity and Conservation*, 14, 1641–1661.
- Zeeberg, J. (1998). The European sand belt in Eastern Europe-and comparison of Late Glacial dune orientation with GCM simulation results. *Boreas-International Journal of Quaternary Research*, 27, 127–139.
- Zhang, X., Friedl, M. A., Schaaf, C. B., & Strahler, A. H. (2005). Monitoring the response of vegetation phenology to precipitation in Africa by coupling MODIS and TRMM instruments. *Journal of Geophysical Research*, 110, 1–14.